UCRL-10816

# University of California

# Ernest O. Lawrence Radiation Laboratory

TWO-WEEK LOAN COPY

*This is a Library Circulating Copy which may be borrowed for two weeks. For a personal retention copy, call Tech. Info. Division, Ext. 5545*

## RECOVERY OF INTERNALLY OXIDIZED SILVER-MAGNESIUM ALLOYS

Berkeley, California

## DISCLAIMER

This document was prepared as an account of work sponsored by the United States Government. While this document is believed to contain correct information, neither the United States Government nor any agency thereof, nor the Regents of the University of California, nor any of their employees, makes any warranty, express or implied, or assumes any legal responsibility for the accuracy, completeness, or usefulness of any information, apparatus, product, or process disclosed, or represents that its use would not infringe privately owned rights. Reference herein to any specific commercial product, process, or service by its trade name, trademark, manufacturer, or otherwise, does not necessarily constitute or imply its endorsement, recommendation, or favoring by the United States Government or any agency thereof, or the Regents of the University of California. The views and opinions of authors expressed herein do not necessarily state or reflect those of the United States Government or any agency thereof or the Regents of the University of California.

UCRL-10816
UC-25 Metals, Ceramics
and Materials
TID-4500 (19th Ed.)

Research and Development

UNIVERSITY OF CALIFORNIA

Lawrence Radiation Laboratory
Berkeley, California

Contract No. W-7405-eng-48

# RECOVERY OF INTERNALLY OXIDIZED SILVER-MAGNESIUM ALLOYS

R. Busch

(Master's Thesis)

June 1963

Reproduced by the Technical Information Division
directly from author's copy

Printed in USA. Price $1.50. Available from the
Office of Technical Services
U. S. Department of Commerce
Washington 25, D.C.

TABLE OF CONTENTS


| | |
|---|---|
| Abstract | iii |
| Introduction | 1 |
| Experimental Procedure | 13 |
| (a) Materials | 13 |
| (b) Specimen Preparation | 14 |
| (c) Apparatus and Techniques | 14 |
| Results | 20 |
| (a) Effect of Internal Oxidation on the Mechanical Behavior at 78°K | 20 |
| (b) Effect of Internal Oxidation on the Electrical Resistivity at 78°K | 23 |
| (c) Strain Dependence of the Electrical Resistivity at 78°K | 23 |
| (d) Annealing Response | 27 |
| Discussion | 38 |
| (a) The Effect of Internal Oxidation on Defect Production During Cold Work | 44 |
| (b) The Effect of Internal Oxidation on the Annealing Response | 48 |
| Summary and Conclusions | 55 |
| Acknowledgments | 57 |
| Figure Captions and Table Captions | 58 |
| Bibliography | 60 |

# RECOVERY OF INTERNALLY OXIDIZED SILVER-MAGNESIUM ALLOYS

R. Busch

Lawrence Radiation Laboratory
and Department of Chemistry
University of California
Berkeley, California

June 1963

## ABSTRACT

The low temperature annealing response of a cold worked internally oxidized silver-0.1 at.% magnesium alloy was investigated and compared with the annealing behavior exhibited by the corresponding solid solution alloy and by pure silver. Wire specimens were deformed in tension at 78°K and the recovery was followed by measurement of the electrical resistivity and flow stress at 78°K after suitable isochronal and isothermal anneals at temperatures between 78° and 550°K.

It has been found that both point defect and dislocation annealing processes are markedly retarded by the presence of the finely dispersed Mg-O clusters introduced by internal oxidation. The effect of the dispersed phase on the annealing behavior is broadly explained in terms of defect cluster interactions. It is suggested that point defect annealing is inhibited because vacancies and/or interstitials generated during plastic deformation are trapped in the strain fields surrounding these clusters. The dispersion provides obstacles to the climb and glide of dislocations and also acts to restrain the motion of grain and subgrain boundaries, thereby retarding the rearrangement and annihilation of dislocations on annealing.

Based on the changes in various physical properties produced by internal oxidation, and evidence obtained from other sources, a model for the structure of the dispersed phase alloy is proposed. The model assumes that coherent clusters or zones of magnesium and oxygen atoms less than 30 Å in diameter are formed in the silver matrix during internal oxidation.

# 1. INTRODUCTION

When a metal is plastically deformed at low temperatures, a part of the energy of deformation is stored in the metal in the form of various structural imperfections, e.g., point defects, point defect aggregates of various kinds, and dislocations. If the metal is then heated, these defects will eventually acquire enough mobility to rearrange themselves into more stable configurations or to anneal out completely. Annealing therefore results in a progressive release of the stored energy of deformation and a return to the defect structure characteristic of the original undeformed state. One of the central problems associated with the mechanical behavior of metals and alloys is to elucidate the nature of the defects present in the cold-worked state, the mechanisms by which these defects are produced and the ways in which they anneal out. The present investigation concerns one fairly specialized aspect of this general problem, namely, the influence which finely dispersed particles of a second phase exert on the annealing response of the cold-worked metal matrix.

Two phase materials of this type have long been of interest because of the great improvement in the strength properties conferred by the presence of the dispersed particles.* A good example is furnished by internally oxidized alloys, which consist of a fine dispersion of oxide particles in a metal matrix. These oxide particles are formed in situ by the selective oxidation of a solute element that has a greater chemical affinity for oxygen

---

*An extensive survey of the literature pertaining to the dispersion strengthening of metals and alloys has been prepared by Bunshah and Goetzel.[1]

than does the base metal. With certain copper, silver and nickel-base alloys, internal oxidation not only leads to a substantial increase in the yield strength at ordinary temperatures but to an even more significant improvement in creep resistance at elevated temperatures. Moreover, softening processes such as recovery and recrystallization appear to be markedly retarded in these materials.[2-4] Gatti and Fullman[4] have found, for example, that the strain hardening introduced by room temperature deformation in an internally oxidized Ag-0.1% Al alloy is retained on annealing up to temperatures as high as 700°C, i.e., to within about 250°C of the melting point of silver; pure silver, on the other hand, recrystallizes at about 100°C under similar conditions.

In view of the magnitude of this effect and its obvious technological importance, it is surprising that relatively few studies of the annealing behavior of dispersed phase materials have been undertaken. Previous work in this area has recently been summarized by Klein.[5] In contrast, however, a great many investigations have been carried out on reasonably pure metals, especially copper, gold and silver. The defects which are formed during low temperature deformation of f.c.c. metals are believed to include vacancies, interstitials, divacancies (and presumably di-interstitials), larger vacancy and interstitial clusters of various types, stacking faults and dislocations. In pure metals and dilute solid solution alloys there is abundant evidence that many of these point defects anneal out at lower temperatures than do dislocations. The typical annealing spectrum which is observed during the progressive heating of cold-worked (also irradiated and quenched) metals such as Cu, Au and Ag is shown schematically in Fig. 1, which was taken from a recent monograph by Van Bueren.[6]

The initial portion of the annealing spectrum is generally found to

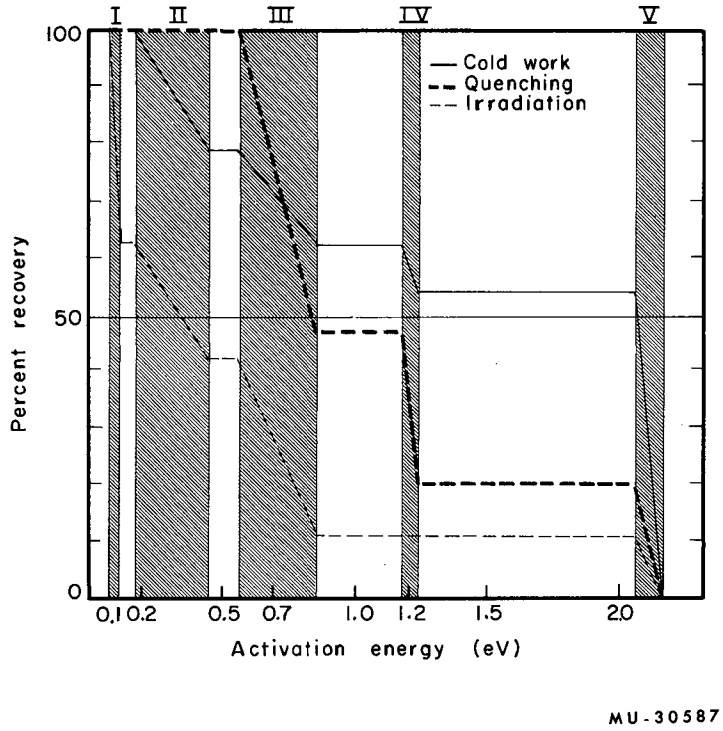


Fig. 1. Schematic representation of the recovery of the electrical resistivity in cold worked, irradiated and quenched noble metals. The various annealing stages I . . . . V are characterized by fairly well defined activation energies. Between stages, some gradual annealing is also observed. (After van Bueren.)

consist of a series of point defect annealing stages (e.g., Stages I, II, III) which are characterized by more or less well defined activation energies. In general, those annealing processes which require the least thermal activation (i.e., those having the lowest activation energies) occur first, followed by higher energy processes as kT becomes sufficiently large. Dislocations may participate in these processes by acting as sinks or trapping centers for point defects and by undergoing small-scale rearrangements. At still higher temperatures, dislocations begin to acquire some mobility and tend to rearrange themselves on a more macroscopic scale by glide (e.g., cross-slip) and climb. Extensive dislocation annealing of this type is generally interrupted, however, by the onset of recrystallization (Stage V in Fig. 1); this process takes place via the migration of high-angle grain boundaries and results in a marked decrease in the average dislocation density.

Balluffi, Koehler and Simmons[7] have recently given a comprehensive and critical survey of the existing state of knowledge concerning point defects and point defect annealing processes in deformed f.c.c. metals. As they and others[6,8] have emphasized, the problem of assigning specific defect mechanisms to the various annealing stages is enormously complicated by the many types of defects and the great variety of interactions between defects which must be considered. This intrinsic difficulty is further compounded by the fact that the details of the annealing spectrum are often extremely sensitive to such experimental variables as the mode, amount and temperature of deformation, the purity of the material, the method of annealing, and the particular physical property or properties being measured. This circumstance makes it especially difficult to compare and evalute the results reported by different investigators. Furthermore, theoretical calculations of the properties of simple point defects (e.g., the energies of formation and migration) are

still sufficiently crude that little guidance can be obtained from theory. It is perhaps not surprising, therefore, that unambiguous assignments have not yet been made except for Stage V, which is universally ascribed to recrystallization.

Considerable progress is being made in this direction, however, by a combination of different approaches, including irradiation and quenching experiments and direct measurements of equilibrium defect concentrations at high temperatures. Nevertheless, Balluffi et al. were forced to conclude in their review that "no (specific) point defect has been positively identified as taking part in any given portion of the annealing spectrum of a cold-worked metal". The present study does not aim at making any detailed mechanistic interpretation of the annealing spectrum; instead, a more modest objective has been chosen. Previous work on the annealing response of dispersed phase materials has been confined exclusively to the temperature range well above room temperature. Although there is clear evidence that dislocation annealing processes (i.e., recrystallization) are strongly retarded by the presence of dispersed particles, almost no information is available regarding the influence of dispersed second phase constituents on point defect annealing processes. The primary intention, therefore, was to determine which of the various low-temperature annealing stages in a pure metal such as silver are influenced by the introduction of a dispersed phase - in this case MgO - and to what extent.

General considerations suggest that the presence of a dispersed phase should modify the annealing behavior of the metal matrix in at least two significant respects. First, to an extent which is dependent upon the nature of the particles, (i.e., their size, shape, spacing, degree of coherency, etc.) the dispersed phase may alter the mode of deformation of the matrix and thus

influence both the type and concentration of the various defects which are produced, as well as the spatial distribution of these defects. Second, the dispersed particles may interact in a variety of ways with point defects and dislocations, so that even if the defect structure of the cold-worked matrix were unchanged by the introduction of the particles, the kinetics of certain annealing stages would still be appreciably altered. It was hoped that the present experiments might make it possible to deduce something about the relative importance of these two effects, as well as the relative influence of the dispersed particles on the kinetics of point defect and dislocation annealing processes.

Convincing evidence that dispersed second phase particles do, in fact, significantly alter the dislocation structure of cold-worked metals has recently been obtained by transmission electron microscopy. Thus, Swann[9] has shown that a fine dispersion of particles may completely prevent the formation of the usual cell structure observed in pure f.c.c. metals. In an internally oxidized Ag-0.1% Al alloy, a pronounced change was noted in the dislocation distribution of the silver matrix. Instead of forming a cell structure, a high density of uniformly distributed, elongated dislocation loops and jogged dislocations were produced. Similar observations have been made by Ashby and Smith[10] on internally oxidized Cu-Al alloys. Prismatic dislocation loops, many of them triangular in shape were seen attached to the $Al_2O_3$ particles, and many of the dislocations were heavily jogged.* Relative to pure silver, Klein[5] has also observed a greater density and uniformity of dislocations in cold-worked internally oxidized Ag-Mg alloys and this has been confirmed indirectly by Fourier analysis of the x-ray line broadening profiles. The high

* The formation of these loops has been explained by Ashby and Smith on the basis of a model wherein the screw components of the matrix dislocations bypass the particles via a double cross-slip mechanism.

initial work hardening rates,[11-13] the absence of easy glide in favorably oriented single crystals[11,14] and the fine surface slip line patterns[14,15] observed in dispersed phase systems are also consistent with the idea that deformation is more homogeneous in these materials and that the distribution of dislocations is substantially more uniform. Direct evidence has also been obtained that dispersed second phase particles provide copious sources for dislocations on quenching[16,17] as well as during plastic deformation.[18] *

It is well established that dislocations interact strongly with dispersed particles and that these particles act as obstacles to the glide motion of dislocations. The strengthening effect associated with the presence of the particles may be broadly understood on this basis, and a number of theories have been proposed to explain dispersed phase strengthening in terms of particle-dislocation interactions.[12,15] However, these theories are sensitive to the details of the assumed interactions, about which relatively little is known, and none of them appear to be completely adequate. The various theories and mechanisms of dispersion hardening have recently been reviewed in detail by Kelly[12] and are also discussed by Guard.[15] Diverse types of particle-dislocation interactions seem possible, depending upon the stacking fault energy of the matrix, the size and spacing of the particles, the crystal structures and elastic properties of the matrix and the dispersed phase,[19] upon whether the particles are coherent, partially coherent or incoherent, deformable or undeformable, etc.

Thus, dislocations moving through the matrix may simply bypass any particles which intersect the glide plane by bowing out between them, leaving

---

* Jackson[20] has recently proposed, moreover, that foreign particles actually provide the real sources for dislocations in crystals grown from the melt.

loops encircling the particles as the dislocation line moves past.[21,22] Alternatively, the dislocations may cross-slip around particles in the manner proposed by Ashby and Smith.[10] If the particles are coherent and if the structures of the particle and matrix are similar, the dislocations may intersect or cut through the particles instead.[12] This type of behavior has been observed, for example, by Nicholson et al.[23] in precipitation-hardened Al-Cu alloys. Particle-dislocation interactions may be studied directly by carrying out deformation experiments on thin foils inside the electron microscope. As yet, however, too few systems have been investigated in this manner to establish the general conditions under which a given type of interaction will be favored.

The outstanding creep resistance of many dispersed phase materials furnishes some clues regarding the nature of dislocation-particle interactions at high temperature. Since the creep rate is believed to be controlled by the climb of dislocations, at least under certain conditions, it appears that dispersed particles must somehow act as obstacles to climb as well as to glide. This problem has been considered in some detail by Weertman[24] who has derived theoretical expressions for the creep rate of dispersion hardened alloys. Again, the predictions are sensitive to the details of the assumed particle-dislocation interactions[13,15] and the theoretical models have not been adequately tested. Nevertheless, the concept that climb is inhibited by the presence of dispersed particles is consistent with the observation that large-scale dislocation annealing is also retarded in such materials.

The situation with respect to the production of point defects in dispersed phase materials is very obscure. There is little doubt that point defects are formed in appreciable numbers in pure metals as a result of low temperature deformation,[6-8] but the degree to which point defect production processes may be influenced by dispersed particles is completely unknown. The

model currently favored for defect production at moving dislocations considers that point defects are created by the non-conservative motion of jogs on dislocations having a strong screw component.[7,25] The nature of the defects produced depends upon many factors, e.g., the actual jog configuration, the Burgers vector of the jog, whether or not jog motion is aided by thermal fluctuations, etc. So far, no attempt has been made to examine the effect of dispersed particles on jog dynamics. It would be expected, however, that the presence of coherency strain fields around the particles or strain fields arising from differential thermal contraction between the particle and the matrix[26] might have an important bearing on the jog production process. In this connection, the heavily jogged dislocations seen in internally oxidized alloys by Swann[9] and by Ashby and Smith[10] may be significant.

One other piece of information of an indirect nature may be mentioned here. Peiffer[27] has determined the strain dependence of the electrical resistivity of composite $Ag-Al_2O_3$ alloys* at 78°K. The resistivity increment on deformation at 78°K was found to obey the usual power law expression

$$\Delta\rho = A\epsilon^n$$

where A and n are constants and $\epsilon$ is the strain. However, the value of n obtained for the dispersed phase material was somewhat less than that for pure silver and was found to decrease with increasing volume fraction of alumina. The results indicated that the formation of defects during cold-work is greatly enhanced by the presence of the finely dispersed $Al_2O_3$ particles. Based on a theoretical analysis[28] of the relative contributions of point defects and dislocations to the resistivity increment, Peiffer has concluded

* Prepared by powder metallurgical techniques.

that most of the resistivity increase observed on deformation is associated with the production of dislocations rather than point defects.

There is good reason to suspect that the annealing out of point defects which are generated during cold work may be influenced by dispersed particles. For example, if coherency strain fields exist around the particles, or if internal strains of a similar nature are developed as a result of differential thermal contraction, it is quite possible that vacancies or interstitials formed during deformation may be trapped in their vicinity. Some evidence for the trapping of vacancies at Guinier-Preston zones in various aluminum alloys has recently been presented by Federighi and Thomas.[29] Depending on the size, shape and spacing of the dispersed particles, and the magnitude of their associated elastic strain fields, it is conceivable that the particles may be even more effective trapping centers for point defects than dislocations; this possibility, however, must be regarded as speculative at the moment.

If the particles are completely noncoherent or if the interfacial energy between the particle and the matrix is high, the interface may act as a good sink for vacancies. Grain boundaries have long been known to be effective sinks for vacancies, while more recently Kasen and Polonis[30] have demonstrated that interphase boundaries in quenched Cu-Si alloys also function as efficient vacancy sinks. Furthermore, Resnick and Siegle[31] have shown that the pores or voids developed during the dezincing of α-brass are heterogeneously nucleated at internal surfaces, i.e., at the interface between oxide inclusions and the matrix. The growth of voids or cavities at grain boundaries under creep-rupture conditions also appears to be accentuated by the presence of second phase particles and this has similarly been explained on the basis that the particle-matrix interface represents an efficient sink for vacancies.[31,32]

To summarize briefly, there appear to be valid grounds for believing that the presence of dispersed second phase particles may have a profound influence on the annealing of point defects as well as dislocations in cold-worked metals. In order to determine whether or not this is actually the case, the annealing behavior of a cold-worked internally oxidized Ag-0.1 at.% Mg alloy has been followed over the temperature range from 78°K to about 550°K by measuring, simultaneously, the recovery of the electrical resistivity and the flow stress; for comparison purposes, the low temperature annealing response of pure silver and the unoxidized solid solution alloy have also been investigated under identical conditions. The electrical resistivity is sensitive to the presence of both point defects and dislocations, while the flow stress will only be changed appreciably when substantial alterations in the dislocation structure occur. Hence, at least a crude separation between point defect and dislocation annealing processes can be made by comparing, in the same specimen, the relative changes in the electrical resistivity and the flow stress which are produced by annealing. Both isochronal and isothermal annealing experiments have been carried out in order to evaluate the activation energies associated with certain of the annealing stages observed in these materials.

Internally oxidized silver-magnesium alloys have been selected for study for a number of reasons: 1) A very large strengthening effect is observed in this system[2,33] and the mechanical properties of these alloys have been thoroughly investigated as a function of the oxidizing variables, i.e., temperature, initial solute concentration, oxygen pressure, etc.[33]; 2) Since oxygen diffuses extremely rapidly in silver, and since silver oxide ($Ag_2O$) itself is thermodynamically unstable above about 200°C, internal oxidation can be accomplished readily and conveniently merely by exposing the alloys

to air or oxygen at elevated temperatures; 3) The structures of internally oxidized Ag-Mg had previously been investigated, at least in a preliminary fashion, by conventional replica methods[33] and transmission electron microscopy[5,34]; 4) Concurrent and closely related studies of these same materials had already been undertaken (i.e., dislocation damping, temperature dependence of the flow stress, etc.) and quenching studies were planned.

## 2. EXPERIMENTAL PROCEDURE

The low-temperature annealing behavior of a deformed internally oxidized Ag-0.1 at.% Mg alloy was studied and compared to the annealing response of high purity silver and the corresponding unoxidized alloy under similar conditions. Wire specimens of each material were deformed in tension at 78°K and the progress of annealing was followed by measurements of the electrical resistivity and flow stress. Both types of measurement were carried out at 78°K on the same sample after suitable isochronal or isothermal anneals at temperatures between 78°K and 550°K.

### a) Materials

The silver used had a nominal purity of 99.9999% and contained < 1 ppm oxygen.* Consistent with this purity level, the measured residual resistivity ratio, $\rho_{293°K}/\rho_{4.2°K}$ was found to be approximately 2000. A 0.1 at.% Mg alloy was prepared from this silver by melting in a purified helium atmosphere in a high purity (< 10 ppm total impurities) thoroughly outgassed graphite crucible.+

To obtain specimens suitable for wire drawing, the silver and the alloy were then melted and cast under vacuum (~ $10^{-6}$ mm Hg) in the form of 3 mm dia. rods approximately 12 cm. long. Outgassed high-purity graphite crucibles were again employed and every precaution was taken to minimize contamination by oxygen.

---

* Supplied by Consolidated Mining and Smelting Company of Canada, Ltd.

\+ Supplied by United Carbon Products Company, Bay City, Michigan.

b) Specimen Preparation

The cast rods were drawn down to wires approximately 0.30 mm in diameter without intermediate annealing. Surface contamination was removed by etching in warm dilute $HNO_3$ giving a final wire diameter of 0.25 mm. The pure silver wires were then annealed for 3 hours at 250°C in vacuum ($\lesssim 10^{-6}$ mm Hg); this treatment gave a uniform recrystallized grain size of about 20 μ. One length of the alloy wire was also annealed under these same conditions, the resulting grain size being approximately the same as that for the pure Ag wire. A portion of the recrystallized alloy wire and the remaining length of cold-drawn alloy wire were then oxidized for 4 hours at 600°C at 1 atm. oxygen pressure.* After this treatment, the excess oxygen in solid solution in the silver matrix (i.e., oxygen not combined with Mg) was removed by degassing for 24 hours at 600°C in a vacuum of $10^{-6}$ mm Hg.

Metallographic examination revealed that some grain growth had occurred during oxidation, particularly near the center of the wires. This effect was slightly more pronounced in the wires oxidized in the cold-drawn condition than in wires which had been recrystallized prior to oxidation, however, no significant difference in grain size could be detected between the two groups of oxidized specimens. The average grain diameter was estimated to be about 50 μ.

c) Apparatus and Techniques

The tensile apparatus was designed to permit operation at a constant

---

* According to a calculation based on the work of Meijering and Druyvesteyn only about 15 min. are required for complete oxidation under these conditions.

strain rate and could be classed as a relatively hard machine. The moveable crosshead, to which the upper specimen grip was fastened, was actuated through an appropriate reduction gear by the constant speed chart drive motor of a Leeds and Northrup Speedomax recorder. The load was applied through a long stainless steel pull rod attached to the moveable crosshead, the lower specimen grip being held securely in a stationary position. A linear differential transformer mounted in a calibrated proving ring attached to the pull rod was used to measure the load. The output of this transformer was amplified and fed into the balance circuit of the recorder. In this way a continuous autographic stress-strain record could be obtained. The strain was calibrated by measuring the actual crosshead motion to within ± 0.001" with a micrometer. Using wire specimens 0.25 mm in diameter, a stress sensitivity of 50 $gm/mm^2$ could easily be obtained. This sensitivity was achieved at all stress levels by the use of a suitable zero suppressor.

The grip assembly is illustrated in Fig. 2, together with the arrangement of the current and potential leads for the resistivity measurements. To facilitate carrying out the low temperature annealing operations, the apparatus was arranged so that the specimen and the grip assembly could be enclosed in a cylindrical copper can which could be evacuated through a long stainless steel tube that also housed the pull rod. Tests at liquid nitrogen temperature could then be conducted by immersing the copper jacket in a Dewar and using dry helium as an exchange gas inside the specimen chamber.

Preliminary annealing runs which served to locate the major annealing stages were carried out in fixed temperature baths with the copper jacket removed and the specimens immersed directly in the bath. The temperature and baths employed were: 78°K ($N_2$: b. pt.) 140°K (methyl cyclohexane, m.pt.),

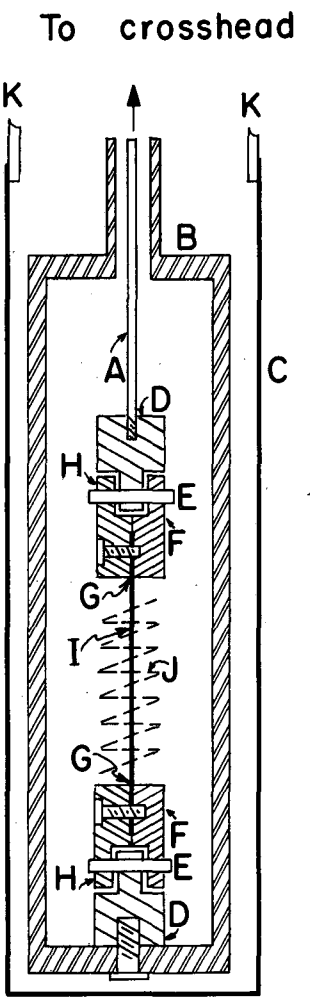


MU-30597

Fig. 2. Schematic illustration of the tensile apparatus, including the cryostat, grip assembly and specimen chamber; (A) Stainless steel pull rod, (B) Stainless steel frame, (C) Copper jacket, (D) Lavite grip holder, (E) Pin fastener, (F) Split specimen grip, (G) Potential lead, (H) Current lead, (I) Specimens, (J) Tungsten heater, and (K) Stainless steel tube.

195°K (dry-ice-acetone), 230°K (ethyl-alcohol-water, m.pt.) and 273°K ($H_2O$, m.pt.). Temperatures between 273°K and 373°K were obtained with a constant temperature water bath. This method of operation was relatively simple but it had several disadvantages. Not only was the choice of annealing temperatures limited, but icing in the low temperature baths made it necessary to warm the specimens essentially to room temperature before cooling back down to 78°K for the flow stress and resistivity measurements. For these reasons, this method of annealing was abandoned in favor of the following procedure.

A helical tungsten ribbon heater was supported concentrically around the specimen (see Fig. 2); this heater was about 1 cm. in diameter and 4 cm. long. With the outer jacket immersed in liquid nitrogen and with helium as an exchange gas inside the specimen chamber, the specimen temperature could be controlled at any desired level between 78° and 550°K by balancing the power input to the heater against the heat loss to the walls of the jacket. Since thermal equilibrium was achieved quite rapidly under these conditions, isochronal anneals as short as 15 minutes in duration could be employed and the specimens could be brought back essentially to liquid nitrogen temperature within a few minutes after the heater current was turned off. With this method of operation, the specimen itself was used as a resistance thermometer. The temperature dependence of the resistivity of silver as given by MacDonald was used to obtain a temperature calibration.

The resistivity apparatus was of the standard potentiometric type in which a constant current, regulated to within 1 part in $10^5$, was passed through the specimen and through a known resistance connected in series. Currents of the order of 0.1 amp were employed. The potential drops across the specimen and the standard resistance were measured with a Rubicon thermo-

free potentiometer (Model 2768) in conjunction with a ballistic galvanometer. Changes in the specimen resistance as small as $1 \times 10^{-6}$ ohm could be detected, which, for specimens of the size employed, corresponds to a sensitivity of approximately $10^{-10}$ ohm-cm. The maximum probable error in the measurement of the resistivity, including the uncertainties in determining the physical dimensions of the specimens, is estimated to be $\pm 5 \times 10^{-9}$ ohm-cm. The resistivity of pure Ag at 78°K was found to be $3.35 \times 10^{-7}$ ohm-cm; this compares very favorably with other values reported in the literature. All measurements were made at 78°K with the specimens incorporated in the tensile apparatus.

Wire specimens having a gauge length of about 4 cm were mounted in the tensile machine in self-aligning split stainless steel grips. Fine copper wires (~ 0.08 mm. dia.) served as potential leads. These were laid cross-wise upon the specimen in the grips and forced into intimate contact with the specimen when the grips were tightened down. This technique was found to give reproducible results without requiring that the leads be soldered or spot welded directly to the specimen. Relatively heavy copper current leads were silver soldered to the ends of the grips, which in turn were electrically insulated from the apparatus by Lavite holders. Insulation of the grips proved to be necessary in order to eliminate parasitic emf's which interfered with the resistivity measurements.

While mounting the wires in the grips, attaching the potential leads and installing the specimens in the apparatus, the grips themselves were clamped rigidly in a special jig so as to minimize accidental bending or deformation of the specimens during handling. All tensile tests and flow stress measurements were carried out at 78°K at a constant strain rate of

$6 \times 10^{-4}$ $sec^{-1}$. Before measuring the resistivity, the load on the specimen was almost completely relaxed, only a small load (approximately 0.5 $kg/mm^2$) sufficient to maintain alignment of the grips being maintained. It was established that this load did not have any influence on the measured resistivity at 78°K.

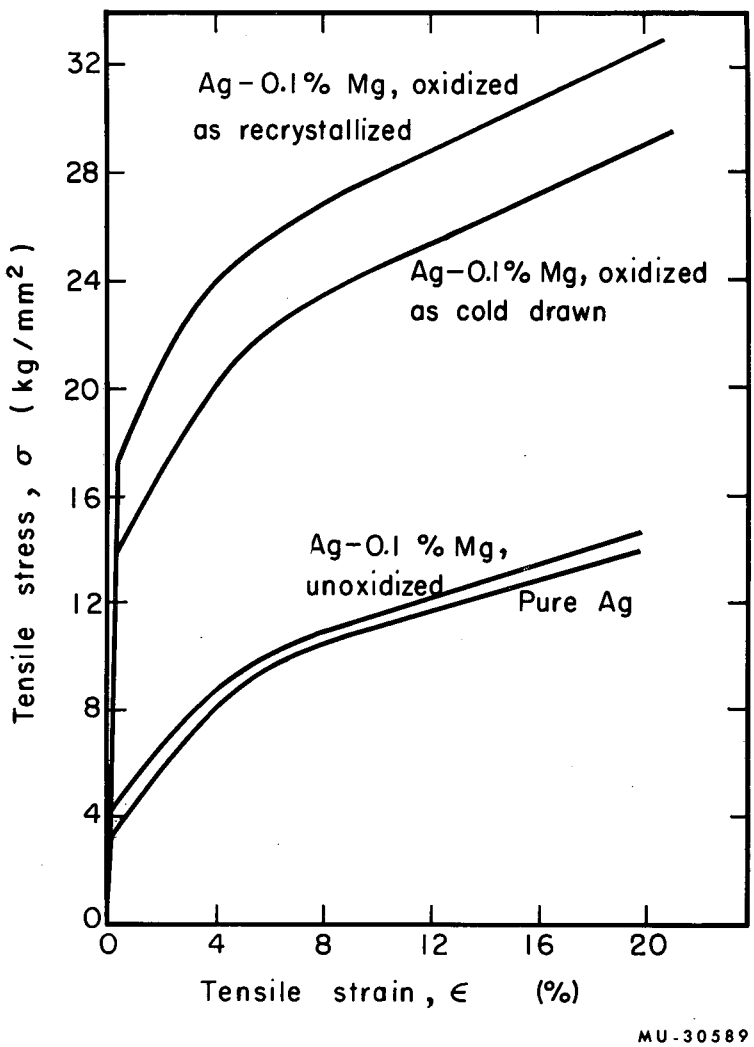


Fig. 3. Representative stress strain curves obtained for internally oxidized Ag-Mg alloys, the corresponding solid solution alloy, and pure silver at 78°K.

## 3. RESULTS

### a) Effect of Internal Oxidation on the Mechanical Behavior at 78°K

Representative stress-strain curves for the different materials are shown in Fig. 3, while values of the initial yield stress and the work hardening coefficients (in the linear hardening range) are listed in Table 1. The potent strengthening effect produced by internal oxidation is shown by the fact that the yield stress of the Ag-0.1% Mg alloy is raised almost by a factor of 4 by oxidizing at 600°C. This strengthening is perhaps even more impressive when it is considered that the volume fraction of oxide in the silver matrix is only about $1 \times 10^{-3}$.

The magnitude of this strengthening effect also appears to be dependent to some extent upon the previous thermal and mechanical history of the material. Thus, specimens oxidized in the recrystallized condition exhibited a consistently higher yield stress than those oxidized directly after cold drawing. This point was checked rather carefully since previous work[33] had indicated that oxidation of cold worked speciments resulted in a greater strengthening effect. The observed difference in yield stress between the groups of oxidized specimens (roughly 3 $kg/mm^2$) was reproducible and was three to four times greater than the scatter in the measurements within each group; hence, it is concluded that the effect is real.

From Fig. 3, it can be seen that, compared to pure silver or to the unoxidized alloy, the internally oxidized specimens exhibit greater work hardening rates at all strains, as in generally observed for dispersion hardened systems. No significant differences in work hardening characteristics were found between specimens oxidized in the cold drawn condition and

Table 1. Mechanical and Electrical Properties of Internally Oxidized Ag 0.1% Mg, the Unoxidized Alloy, and Pure Silver at 78°K

| Material | Yield Stress $kg/mm^2$ | Linear Work Hardening Coefficient | Initial Resistivity, $\rho_o$ $\mu\Omega$-cm | A $\mu\Omega$-cm | n | $\frac{\Delta\rho}{\rho_o}$ $\epsilon=0.2$ | $\Delta\rho$, $\mu\Omega$-cm |
|---|---|---|---|---|---|---|---|
| 99.9999 Ag | 3.2 | 0.33 | 0.335 | 0.56 | 1.54 | 0.152 | 0.051 |
| Ag 0.1% Mg | 4.3 | 0.31 | 0.407 | 0.61 | 1.57 | 0.135 | 0.055 |
| Ag 0.1% MgO(1) | 17.4 | 0.49 | 0.443 | 0.67 | 1.45 | 0.167 | 0.074 |
| Ag 0.1% MgO(2) | 14.1 | 0.54 | 0.498 | 0.31 | 0.75 | 0.182 | 0.091 |

(1) Oxidized as recrystallized

(2) Oxidized as cold drawn

those which had been recrystallized prior to oxidation.

No strain aging effects or unloading yield point effects were observed under any of the testing conditions employed in these experiments.

b) Effect of Internal Oxidation on the Electrical Resistivity at 78°K

Internal oxidation of the Ag-0.1% Mg alloy led to a significant increase in the electrical resistivity, as is shown in Table 1. This increase amounted to about 9% and 22%, respectively, for specimens oxidized in the recrystallized and cold drawn condition, both these values being relative to the initial resistivity of the annealed (i.e., recrystallized) alloy. A similar increase in the resistivity had previously been noted by Meijering and Druyvesteyn[2] and by Gorsuch.[33] At first glance, this behavior seems anomalous since it might have been expected that oxidation would effectively remove magnesium atoms from solid solution, thereby lowering the resistivity. Such is found to be the case, in fact, in all other internally oxidizable systems except Ag-Mg and Ag-Be. The structural implications of this effect are discussed at some length below.

c) Strain Dependence of the Electrical Resistivity at 78°K

The increase in the electrical resistivity produced by tensile deformation at 78°K is shown in Fig. 4, in which the resistivity increment is plotted as a function of the strain on a log-log scale. It is seen that, for all the materials investigated, the dependence of the resistivity increment on strain is well described empirically by a power law expression of the form:

$$\Delta \rho = A \epsilon^{n},$$

where A and n are constants. This is the behavior commonly observed with polycrystalline f.c.c. metals deformed at low temperatures.

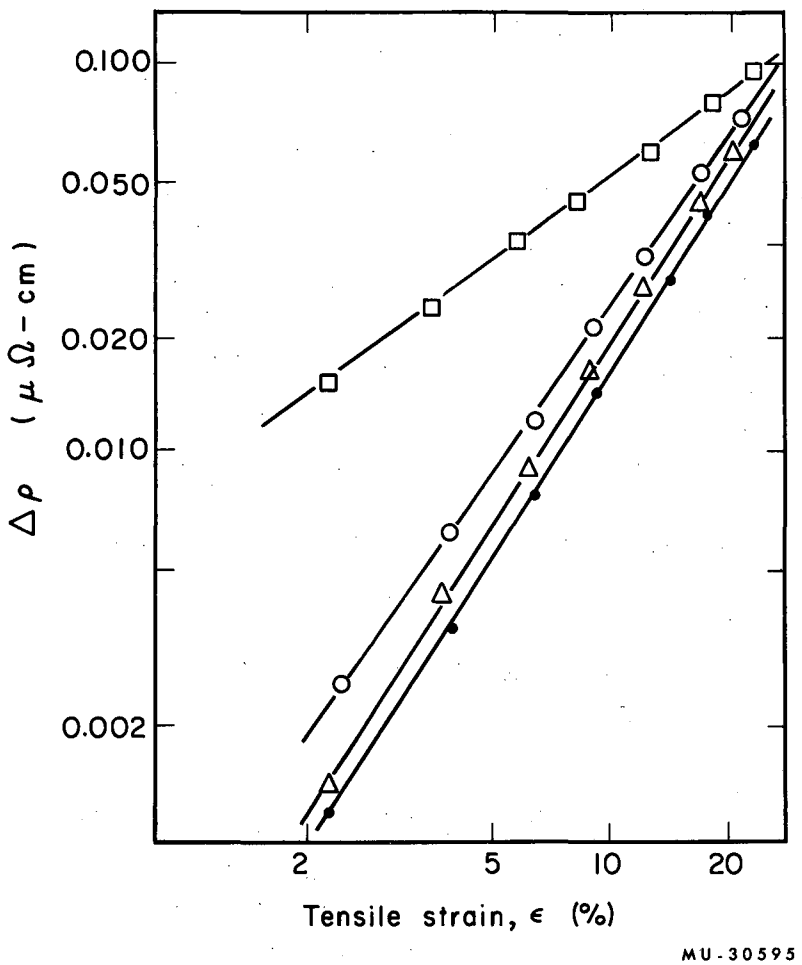


Fig. 4. The strain dependence of the electrical resistivity at 78°K for the four materials shown in Fig. 3.

The values of A and n derived from Fig. 4 are listed in Table 1. For pure Ag, the solid solution alloy, and the alloy oxidized in the recrystallized condition, the exponent n lies in the range from 1.45 to 1.57. These values are in reasonable agreement with those (1.15 to 1.53) previously reported in the literature[6] for 99.98 - 99.99% pure Ag deformed at 78°K. However, the alloy oxidized in the cold drawn state showed a distinctly different behavior; for this material the exponent n was approximately 0.75. The qualitative difference in the strain dependence of the resistivity exhibited by this material, compared to the other specimens, is shown more clearly in Fig. 5, where $\Delta\rho$ is plotted as a function of the strain on a linear scale. It is seen that a value of $n < 1$ for the alloy oxidized in the cold drawn condition corresponds to a continuously decreasing $d\,\Delta\rho/d\epsilon$, whereas $n > 1$ for the other materials corresponds to a continuously increasing $d\,\Delta\rho/d\epsilon$. Possible interpretations of this behavior are considered in the discussion.

For comparison purposes, the values of $\Delta\rho$ and $\Delta\rho/\rho_o$ ($\rho_o$ = resistivity at $\epsilon$=o) corresponding to 20% strain at 78°K are also listed in Table 1. This was the initial strain which each specimen received before annealing. At $\epsilon$=0.20 the increment in the resistivity produced by deformation was substantially greater in the oxidized specimens than in the solid solution alloy or in pure Ag. As will be discussed, this implies a higher rate of defect production in the oxidized materials. The greatest increase in the resistivity on deformation was exhibited by the alloy oxidized in the cold drawn state, this behavior being even more pronounced at lower strains, (see Figs. 4 and 5).

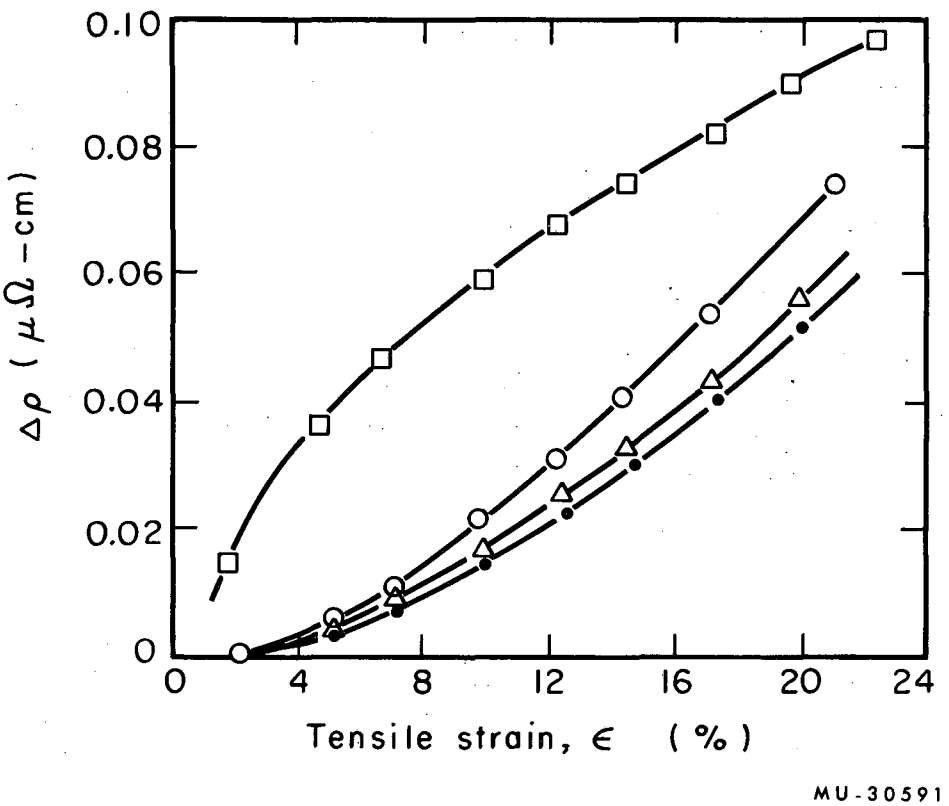


Fig. 5. The strain dependence of the electrical resistivity at 78°K; same as Fig. 4 except plotted on a linear scale.

d) Annealing Response

1. Recovery of the Electrical Resistivity on Annealing

The preliminary annealing runs in fixed temperature baths yielded the isochronal annealing curves shown in Fig. 6. The data have been normalized by plotting $\Delta\rho_T/\Delta\rho_{78°K}$ as a function of the annealing temperature, $\Delta\rho_T$ being the resistivity increment after a 1/2-hour anneal at each indicated temperature T, and $\Delta\rho_{78°K}$ being the resistivity increment observed at 78°K immediately after a 20% strain. Although only a few widely spaced anneals were carried out, it is evident that considerably less recovery of the resistivity occurred in the oxidized specimens than in pure silver or in the unoxidized alloy over the entire temperature range investigated. Two distinct annealing stages are observed in pure silver, one centered around 100°K and the other around room temperature. These same recovery stages are also present in the solid solution alloy but appear to be displaced somewhat toward higher temperatures as expected. In contrast, there is only a vague indication of a recovery stage between 150° and 200°K in the alloy oxidized in the recrystallied condition, while the oxidized cold drawn alloy exhibits essentially continuous background annealing without any evidence of a distinct recovery stage up to 373°K.

Considerably better definition of the low temperature annealing stages was achieved in the second set of isochronal annealing experiments which were carried out in the cryostat using the tungsten heater. In these experiments the isochronal annealing time was reduced to 15 minutes. The results, which are shown in Fig. 7, are seen to be in qualitative accord with the previous 30-minute isochronal annealing data. The two recovery stages in pure Ag and in the solid solution alloy are clearly evident; these two stages appear to be separated by a temperature range in which the background annealing is more

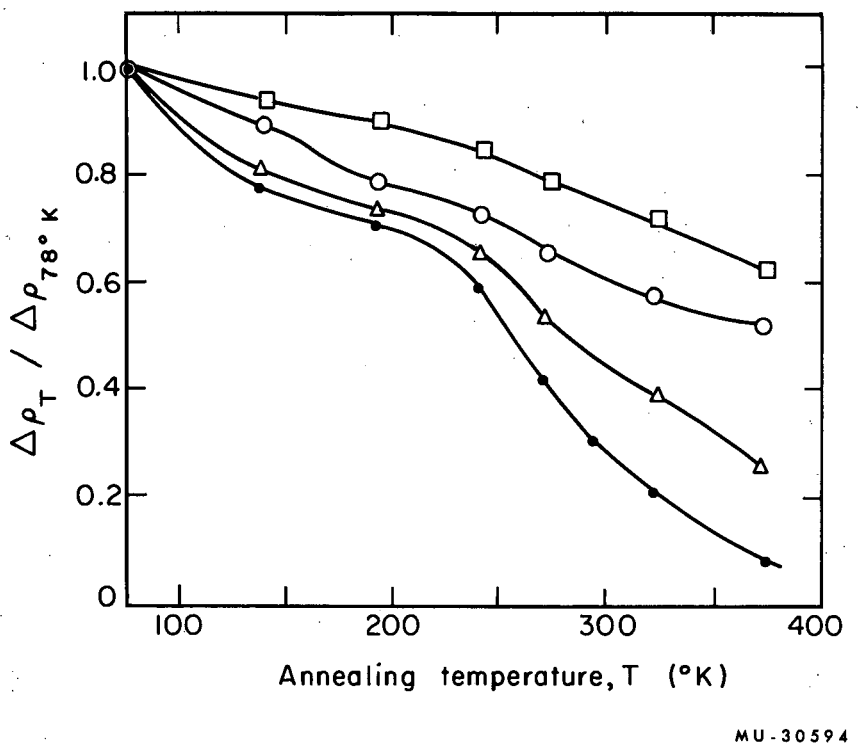


Fig. 6. Isochronal annealing response after 20% tensile deformation at 78°K. The fraction of the initial resistivity increment (normalized) remaining after each successive anneal is plotted as a function of the annealing temperature. Holding time at each point equals 15 min.

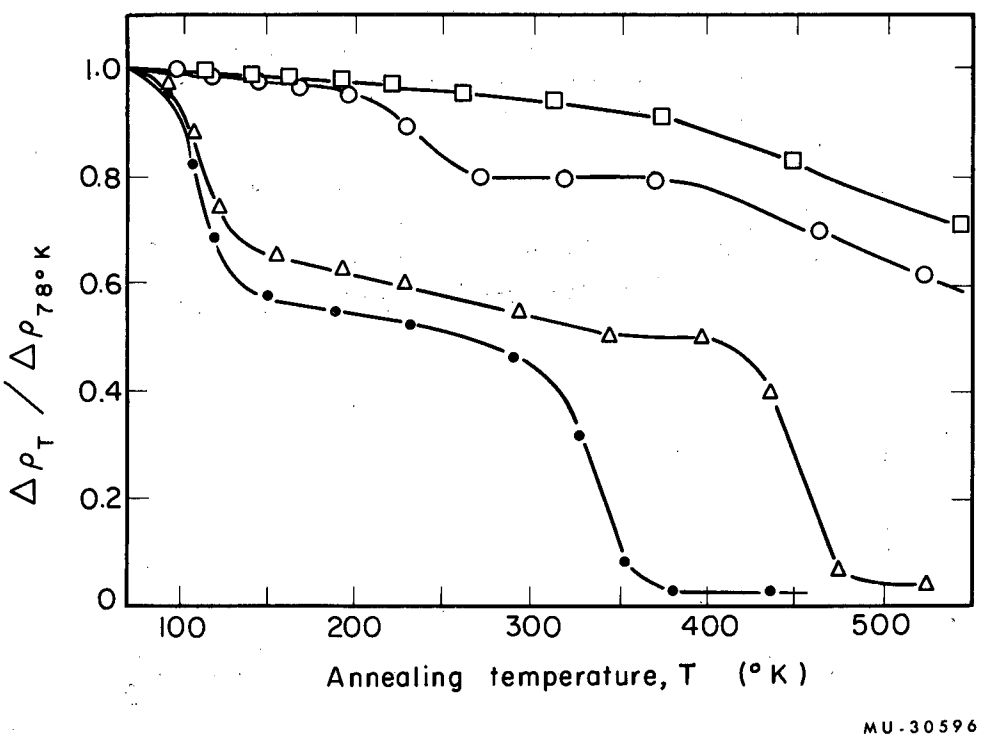


Fig. 7. Isochronal annealing of the electrical resistivity; same as Fig. 6 except holding time at each point equals 30 min.

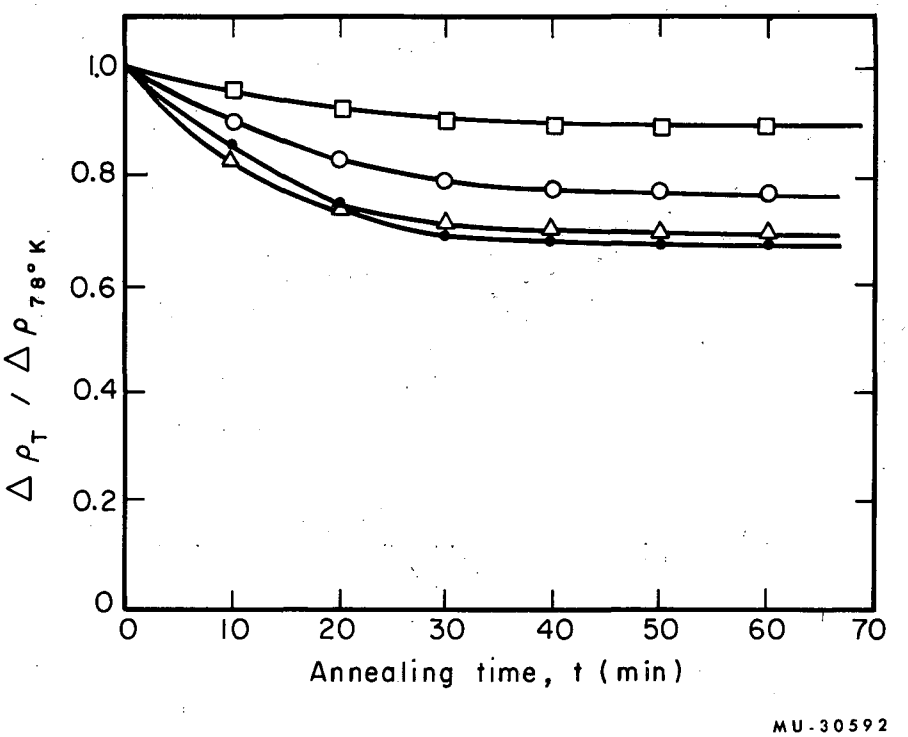


Fig. 8. Isothermal annealing of the electrical resistivity at 195°K.

or less continuous. The first annealing stage, which corresponds to Stage II in the notation used by Van Bueren, occurs between 90° and 130°K in both pure Ag and the unoxidized Ag-Mg alloy; this stage accounts for about 40% of the total recovery in pure silver and about 30% in the alloy. The second annealing stage occurs between 300° to 360°K in pure silver and between 410° and 475°K in the solid solution alloy. It is believed that this stage corresponds to recrystallization in both materials and is therefore designated as Stage V. The recovery of the electrical resistivity which occurs in Stage V accounts for between 45 and 50% of the total recovery in both materials.

The oxidized specimens exhibit essentially no recovery (< 5%) up to 190°K. Between about 190° and 275°K, a fairly well defined annealing stage occurs in the alloy specimens which were recrystallized prior to oxidation, the recovery in this stage amounting to about 15% of the initial resistivity increment; however, this stage is absent in specimens oxidized in the cold drawn condition. The latter exhibit a broad continuous annealing spectrum with no observable fine structure up to the highest temperatures investigated (~550°K). The total recovery obtained on isochronal annealing up to 500°K was only about 25% in the oxidized cold drawn specimens and about 35% in the specimens which were recrystallized before oxidation; the corresponding amount of recovery in pure Ag and in the unoxidized alloy was 95-98%.

A series of isothermal anneals were also carried out at 78°, 195° and 273°K. Within the sensitivity of the measurements, no recovery was observed in the oxidized materials at 78°K in times up to 24 hours. With pure Ag, and the unoxidized alloy about 2% of the initial $\Delta\rho$ annealed out at 78°K during the first 15 minutes but essentially no further annealing took place thereafter. The results of the isothermal annealing runs at 195° and 273°K

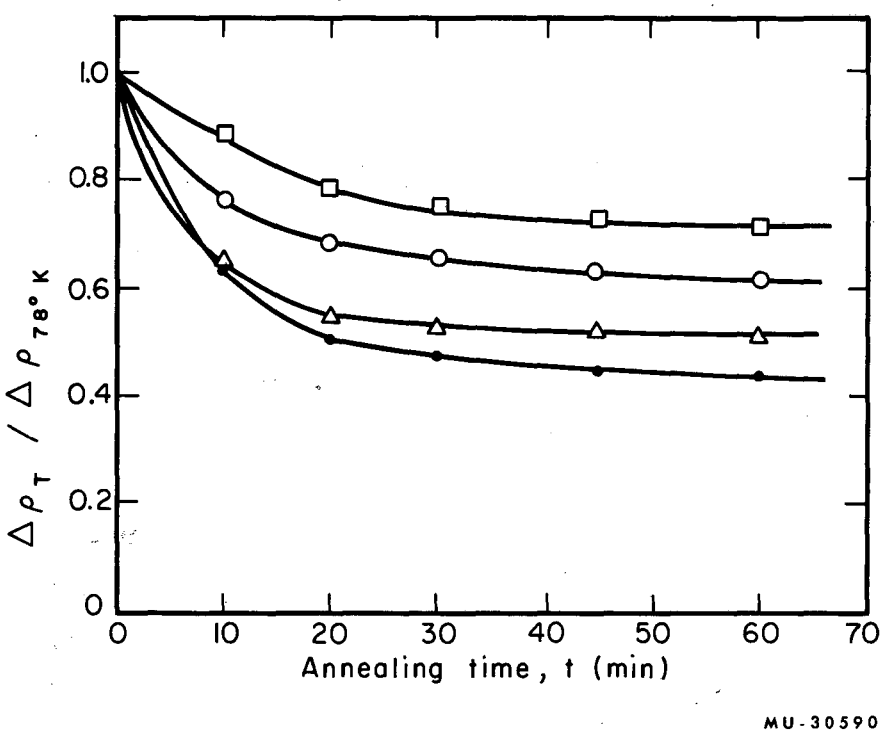


Fig. 9. Isothermal annealing of the electrical resistivity at 273°K.

are presented in Figs. 8 and 9, respectively. At both temperatures the initial rate of recovery is significantly lower in the oxidized specimens than in pure silver or in the solid solution alloy and the total amount of recovery is also appreciably lower in the internally oxidized specimens. The initial recovery rates at 195° and 273°K are found to increase in the following order: oxidized cold drawn alloy, oxidized recrystallized alloy, pure silver, unoxidized solid solution alloy. During the early portion of the annealing process the unoxidized alloy appears to recover slightly faster than pure silver; however, after longer times the total recovery is greater in pure silver. This same effect is observed both at 195° and 273°K, but since the difference in the initial recovery rate is small and possibly within the scatter in the measurements, it may not be significant. In general, therefore, the isothermal annealing behavior appears to be entirely consistent with the results of the isochronal annealing runs.

Having both isochronal and isothermal annealing data for initially identical specimens, it is possible to determine the activation energy, E, associated with a given annealing stage using the analysis developed by Meechan and Brinkman,[36] namely,

$$\ln \Delta t_i = \text{const} - E/KT_i$$

where $\Delta t_i$ is the increment of isothermal annealing time required to produce the same resistivity change as is observed in the $i^{th}$ isochronal annealing pulse at temperature $T_i$. The Meechan-Brinkman analysis was applied to the data obtained for Stage II in both pure silver and the solid solution alloy and to the stage observed in the alloy oxidized in the recrystallized condition. A representative plot of $\ln \Delta t_i$ vs. $1/T_i$ for pure Ag is shown in Fig. 10. The same activation energy was obtained for all three annealing stages

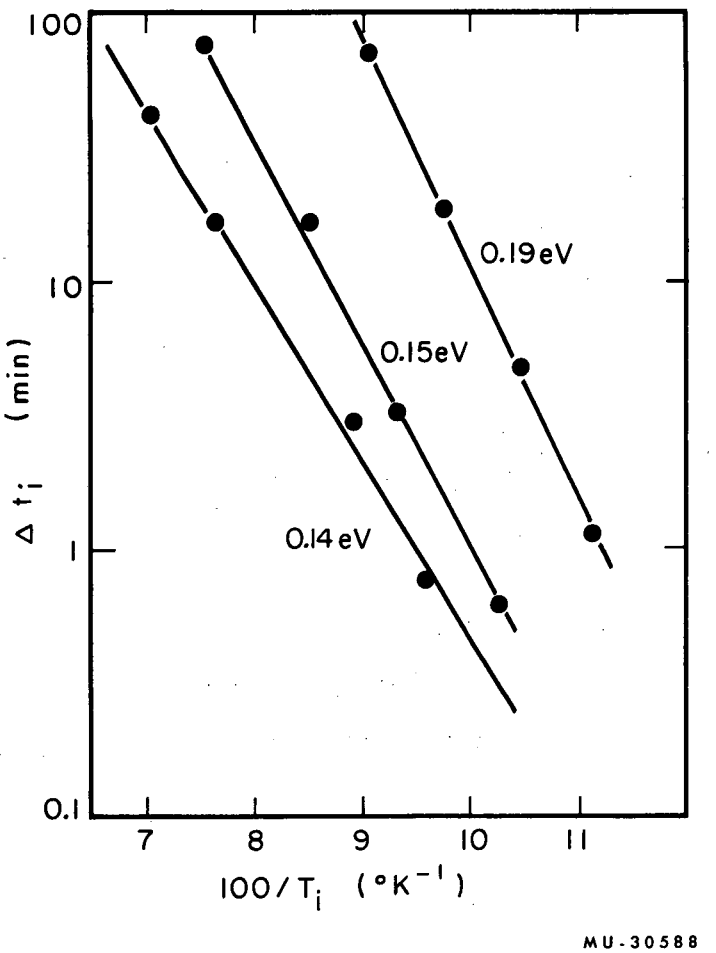


Fig. 10. Isochronal annealing of the flow stress. The fraction of the initial strain hardening increment at 78°K (normalized) remaining after each successive anneal is plotted as a function of annealing temperature. Holding time at each point equals 15 min.

mentioned above, namely 0.16 ± 0.03 eV. This is taken as evidence that the process occurring in the 190° - 275°K recovery stage in the oxidized alloy is basically the same as that in Stage II in pure silver and in the unoxidized alloy. The activation energies corresponding to Stage V in pure Ag and the solid solution alloy could not be evaluated with confidence and hence are not reported.

Attempts were also made to establish whether or not the isothermal annealing processes could be described by either first or second order kinetics. First order reaction kinetics are indicated if $\ln \Delta\rho$ remaining at time t varies linearly with t, while second order kinetics are obeyed if $1/\Delta\rho$ varies linearly with t. These tests, applied to the isothermal annealing data at 195° and 273°K, showed that integral order kinetics were not obeyed; instead, kinetics of fractional order near unity seem to be indicated. This result is understandable since the isothermal annealing temperatures employed do not lie within the temperature range of the major annealing stages; thus, it is likely that at 195° and 273°K, two or more defect annealing processes are taking place simultaneously and, if so, simple kinetics would not be expected.

2. <u>Recovery of the Flow Stress on Annealing</u>

The isochronal annealing of the flow stress (15 minute holding time at each temperature) is shown in Fig. 11. The data have again been normalized by plotting the fraction of the initial flow stress increment (corresponding to $\epsilon = 0.20$ at 78°K) remaining after each succeeding isochronal anneal against the annealing temperature. Pure silver and the unoxidized alloy are seen to exhibit little recovery of the flow stress until temperatures corresponding to Stage V in the respective materials are reached. Furthermore, softening

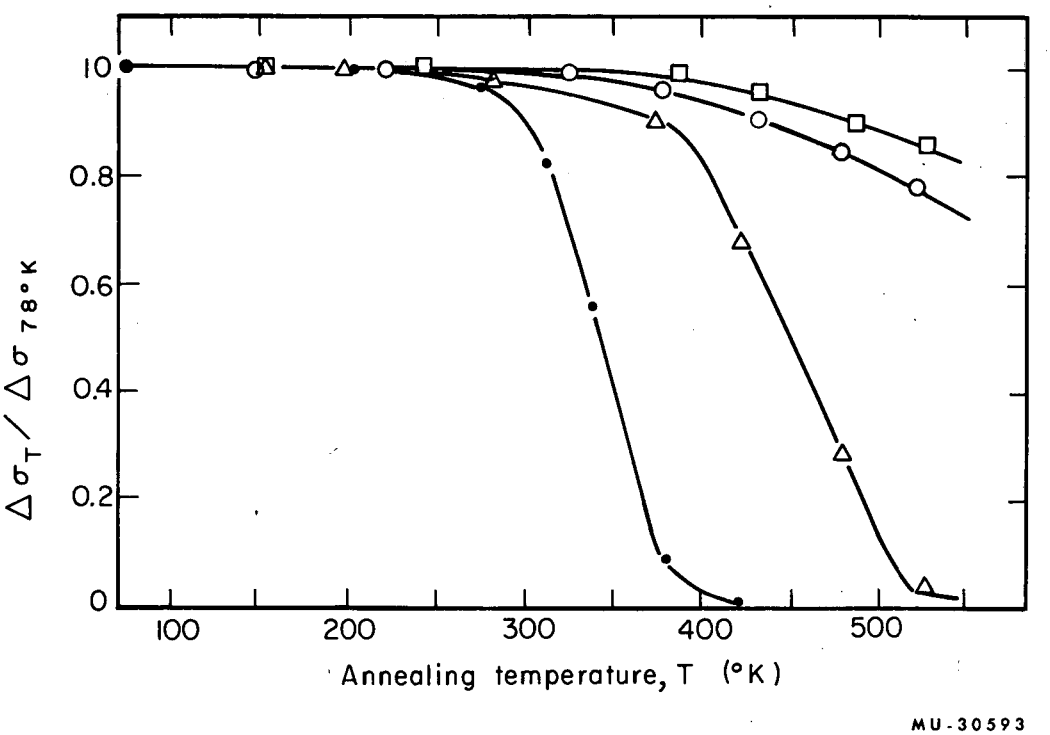


Fig. 11. Determination of the activation energy for Stage II in pure Ag. Each plot corresponds to a different specimen deformed and annealed under similar conditions.

is essentially complete at the end of this stage. This constitutes a strong argument in favor of assigning this stage to recrystallization.

In contrast, the first sign of softening in the oxidized alloys does not manifest itself until about 400°K, a temperature well above that at which pure silver recrystallizes. In general, the recovery of the flow stress proceeds much more gradually in the oxidized materials so that even at 550°K about 80% of the initial strain hardening still remains. It will also be noted that softening occurs less rapidly in specimens oxidized in the cold drawn condition than in the specimens which were recrystallized prior to oxidation. This behavior parallels quite closely that observed during isochronal annealing of the electrical resistivity.

## 4. DISCUSSION

To provide a firmer basis for interpretation of the annealing experiments, a structural model will first be presented for the internally oxidized alloys. In essence, the proposed model is similar to that recently suggested by Darken[37] for the Ag-Al-O system, its principal feature being that during internal oxidation small clusters of magnesium and oxygen atoms, perhaps no more than 30 Å in diameter, are formed coherently with the silver matrix. From a structural standpoint, these clusters are believed to be similar in most respects to the Guinier-Preston zones observed during the early stages of precipitation in supersaturated solid solution alloys such as Al-Ag and Al-Cu. The evidence supporting this model will now be reviewed.

The observed increase in the electrical resistivity on oxidation (see Table 1) together with the fact that the average dislocation density is not changed appreciably by oxidation[37] implies that the silver matrix is heavily strained. This strain contribution to the resistivity must, in fact, outweigh the decrease in the resistivity expected as a result of the precipitation of magnesium atoms from solid solution.* Additional evidence that the silver matrix is elastically strained is provided by the following observations: 1) the lattice parameter also increases on oxidation;[2,33] 2) there is a pronounced broadening of the x-ray reflections;[5,33,38] 3) protuberances are seen on the surfaces of oxidized specimens which seem to represent the extrusion of entire grains above the surface;[37,39] this effect is not observed when pure silver is oxidized under the same conditions.

---

* The increase in the resistivity on oxidation cannot be accounted for by the presence of oxygen in solid solution since the uncombined oxygen had previously been removed by vacuum outgassing.

It is believed that elastic strains arise largely as a result of the formation of coherent clusters or zones of magnesium and oxygen atoms in the silver matrix. The crystal structures and unit cell dimensions of silver and MgO are illustrated for comparison purposes in Fig. 12. It may be seen that the NaCl-type structure of MgO is simply derived from that of silver by substituting magnesium atoms for silver and placing oxygen atoms in the octahedral interstices in the f.c.c. silver lattice. Moreover, the lattice constants of MgO and silver (at room temperatures) differ by less than 3%. This close structural similarity makes it appear highly probable that coherency exists between these two phases, especially when the Mg-O clusters or zones are extremely small. In this connection, it may be noted that thin single crystal films of silver may be produced by epitaxial growth on the surfaces of rocksalt crystals and that these films are indeed coherent with the substrate.[40]

Since the bulk thermal expansion coefficients of silver ($18 \times 10^{-6}/°C$) and MgO ($10 \times 10^{-6}/°C$) differ appreciably, it is also possible that elastic strains will be set up around the MgO clusters as a result of differential thermal contraction. Any such strains would contribute to the resistivity in the same way as coherency strains, and the effects would be difficult to distinguish. However, considering the fact that the internally oxidized alloys were slowly cooled ($< 50°C/hr$) from 600°C, which should have allowed some opportunity for the internal stresses developed on cooling to relax, it is felt that the strain contribution from this source is probably small in comparison to the effects of coherency. It is interesting to note that Ashby and Smith[10] have observed coherency strain fields surrounding $\gamma$-$Al_2O_3$ particles in internally oxidized Cu-Al alloys. The oxide particles in this case are actually plates lying on (111) planes with their edges parallel to < 110 >

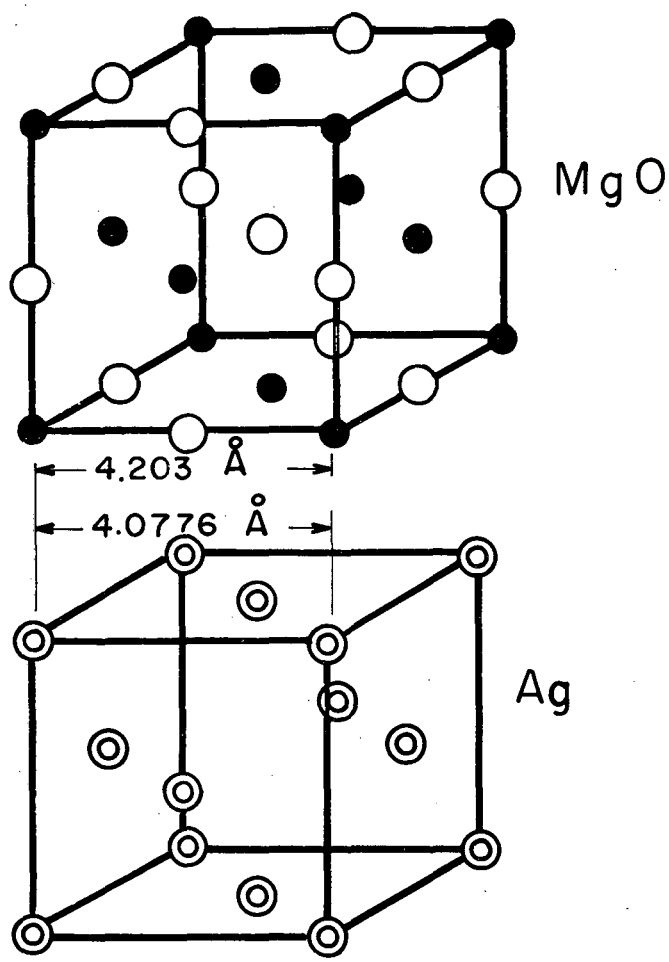


MU-30586

Fig. 12. Comparison of the crystal structures and unit cell dimensions of MgO and Ag, showing the similarity in atomic positions and the small degree of mismatch of the two lattices.

directions in the copper matrix.* In internally oxidized Cu-Si alloys, however, no strain fields were seen around the spheroidal $SiO_2$ particles, the matrix-particle boundary being completely noncoherent.

Thin film transmission microscopy of internally oxidized Ag-Mg alloys has so far failed to reveal the presence of distinct oxide particles, nor have any contrast effects been observed which could definitely be attributed to coherency.[5,34] The absence of resolvable particles indicates that the clusters of magnesium and oxygen atoms formed during oxidation must be less than 30 Å in diameter and probably considerably smaller. Swann and Wreidt[41] have examined the structures of internally oxidized Ag-Al alloys by transmission electron microscopy and have established an upper limit of 30 Å for the size of the Al-O clusters in this material; this figure most likely represents an overestimate since it includes the associated strain field as well. Small angle x-ray scattering measurements likewise indicate that the average cluster size is less than 30 Å.[38] Thus, there appears to be a close structural similarity between the Ag-Al-O and Ag-Mg-O systems. However, since the clusters are not resolvable, or just barely so, it is not possible to establish their shape or to decide with certainty whether or not they are coherent.

The small size of the Mg-O clusters formed during internal oxidation may be understood on the basis of the following considerations. Oxygen diffuses extremely rapidly in silver[42] compared to magnesium. At 600°C, for example, the two diffusion coefficients probably differ by four or five orders of

---

* The geometrical conditions for coherency appear to be even more favorable in the Ag-Mg-O system than in Cu-$\gamma Al_2O_3$.

magnitude.* Because of the strong chemical affinity between the two solute elements, oxygen atoms diffusing in from the surface rapidly seek out and combine with magnesium atoms before the latter have had an opportunity to migrate many atomic distances. Once this happens, the distribution of magnesium and oxygen in the silver matrix is effectively 'frozen in' since pairs or larger aggregates of magnesium and oxygen atoms are immobile. The only way this distribution can be changed is by thermally dissociating the magnesium and oxygen atoms within a given cluster, and then having both constituents diffuse individually to other clusters in the vicinity. This growth process should be very sluggish, however, due to the large binding energy between magnesium and oxygen atoms, which amounts to several eV. In keeping with these ideas, it is well known that the dispersions produced by internal oxidation of dilute silver alloys are extremely stable and do not tend to coarsen appreciably even on prolonged heating near the melting point. The average number of magnesium atoms in clusters formed on oxidation may thus be determined to a large extent by the initial distribution of magnesium atoms in solid solution prior to oxidation. Since silver and magnesium have nearly the same atomic radii, extensive clustering would not be expected, especially at concentration as low as 0.1 at. %.

One other possibly significant factor may be mentioned. It is generally believed that oxygen dissolves interstitially in silver and that the diffusion of oxygen occurs by an interstitial mechanism.** [42] If so, oxygen must

---

* The tracer diffusion coefficient for magnesium has not been measured directly but it should have a value close to that for other divalent substitutional solutes in silver.[43]

** This is based to a large extent on the high diffusivity of oxygen. The activation energy for diffusion of oxygen in silver is only 0.48 eV[42] as compared to about 2.0 eV for substitutional solutes.[43]

exist as essentially neutral atoms, since the $O^{=}$ ion is normally far too large to be accomodated in interstitial positions in the silver lattice. However, when a neutral oxygen atom jumps into an interstitial site adjacent to a magnesium atom, both the oxygen and the nearest neighbor magnesium should become strongly ionized since this approximates the type of bonding which exists in MgO. The oxygen is now trapped in an interstitial position, not as a neutral atom but essentially as an $O^{=}$ ion. A very large matrix strain would therefore result. This strain might be reduced by forming larger MgO clusters.

### a) The Effect of Internal Oxidation on Defect Production During Cold Work

The stress-strain curves for the oxidized alloys exhibit the usual features characteristic of dispersion hardened materials, namely, a significantly higher yield stress and a greater strain hardening rate relative to the solid solution alloy or pure silver. In general, the resistivity increment produced by deformation is also considerably greater in the oxidized materials. Neglecting, for the moment, the differences between the two groups of oxidized specimens, it seems safe to conclude from these results that higher concentrations of defects are generated by cold work in the oxidized materials than in pure silver or the unoxidized alloy. Unfortunately, the nature of these defects cannot be established unambiguously from these experiments. Some order-of-magnitude calculations of the defect concentrations can be made, however, based on the theoretical scattering cross-sections of dislocations and point defects.

For example, at $\epsilon = 0.20$, $\Delta\rho = 0.074$ $\mu\Omega$-cm for the alloy oxidized in the recrystallized condition, while for pure silver, $\Delta\rho = 0.051$ $\mu\Omega$-cm (see Table 1). Taking the reported theoretical values for the resistivity increment per unit length of dislocation in silver, which range from $1.3 - 3.6 \times 10^{-13}$ $\mu\Omega$-cm/cm dislocation line/cm$^3$,[6,8,44] it is found that an excess dislocation density of about $1 \times 10^{11}$ cm/cm$^3$ would account for the entire difference in the resistivity increment between these two materials. Bailey and Hirsch[45] have estimated the dislocation densities in deformed 99.99% silver by measuring the total projected length of dislocation line per unit area on transmission micrographs of foils of known thickness. They give a dislocation density of $5 \times 10^{10}$ cm/cm$^3$ after 20% elongation. Thus, to explain the observed resistivity increment in the oxidized alloy, the dislocation density would have to be about $1.5 \times 10^{11}$ cm/cm$^3$, i.e., roughly a factor of three greater than that in

pure silver.* The observations by Swann[9] show that this is not unreasonable; furthermore, Klein[5] has found, from an analysis of x-ray line broadening profiles, that the dislocation density is between 2-5 times higher in internally oxidized Ag 0.1% Mg alloys than in pure silver after 75% reduction by rolling.

It is also possible to assign part of the resistivity increment to the creation of point defects during deformation. Most theoretical calculations indicate that the resistivity change due to monovacancies (in copper) is about 1.0±0.5 μΩ-cm/at. % vacancies, and that the scattering associated with interstitials is at least as high or higher.[6,7,8] As will be discussed in greater detail below, the annealing behavior of pure silver indicates that roughly 50% of the resistivity increment on deformation may be associated with the introduction of point defects. This corresponds to a point defect concentration of about $1 \times 10^{19}/cm^3$, which is well within the range of theoretical estimates based on jog production models.[6] However, the assumption that even greater concentrations of point defects are generated in the oxidized material than in pure silver leads, as will be seen, to certain difficulties in the interpretation of the annealing experiments.

The strain dependence of the resistivity increment provides some additional clues concerning the defect structures of these materials. It is seem from Figs. 4 and 5 that pure silver, the solid solution alloy, and the alloy oxidized in the recrystallized condition all exhibit virtually the same behavior. For all these materials, $\Delta\rho \propto \epsilon^{3/2}$ and the resistivity increment per unit strain

---

* It is also conceivable that when distributed on a more uniform scale, as in the deformed oxidized alloys, dislocations make a greater effective contribution to the resistivity than when arranged in the form of dense tangles within cell walls, as in cold-worked silver.

increases with increasing strain. This behavior is characteristic of pure f.c.c. metals[6] and indicates that essentially the same mechanisms of defect production are operative in the oxidized alloy as in pure silver, although the relative concentrations of dislocations and point defects which are produced may be substantially different in these two materials.

On the other hand, the behavior of the alloy oxidized in the cold drawn condition appears quite anomalous. In this material $\Delta \rho$ is proportional to $\epsilon^{3/4}$ instead of $\epsilon^{3/2}$ and the resistivity increment per unit strain decreases with increasing strain. If the arguments given by van Bueren[6,28] and Peiffer[27] are valid, the $\epsilon^{3/4}$ strain dependence implies that the dislocation contribution to the resistivity far outweighs that due to point defect production in this material. The absence of a well defined annealing stage (see below) attributable to point defects in this alloy is also consistent with this interpretation.

The rather pronounced differences in the strain dependence of the resistivity between the two groups of oxidized specimens can be explained in the following way. When the alloy wires are oxidized in the cold drawn condition, the dislocation structure produced by wire drawing is partially retained. This is because the oxidation process occurs so rapidly in the surface layers that the dislocations in this region are effectively pinned before they have an opportunity to anneal out.[33] Although recrystallization does take place in the center of the cold drawn wire before oxidation is completed, as shown by metallographic examination, the average density of dislocations in the oxidized as cold drawn material is undoubtedly somewhat higher than that in samples which had been recrystallized prior to oxidation. This agrees with the observation that the resistivity increment produced by oxidation is substantially greater in the cold drawn specimens (see Table 1).

The high initial density of dislocations in the surface layers of the cold drawn and oxidized wire would be expected to modify the deformation behavior quite significantly. For example, since these dislocations are probably pinned at various points along their length by Mg-O clusters, they could well act as Frank-Read sources. A higher source density implies a higher initial rate of production of dislocations and would also account for the greater resistivity increment observed on deformation. To be consistent the initial work hardening rate should also be greater; this is actually observed (Table 1) although the effect is small, and possibly not significant.

## b) The Effect of Internal Oxidation on the Annealing Response

The annealing behavior of the oxidized alloys will now be compared with that of pure silver and the corresponding solid solution alloy. To provide a basis for comparison, the results obtained for pure silver will first be discussed in relation to the work of previous investigators. The manner in which the annealing behavior of silver is modified by the introduction of the dispersed phase will then be considered, and finally, an attempt will be made to rationalize the observed differences between the two groups of oxidized specimens.

Previous work on the low temperature annealing behavior of cold worked silver is summarized in Table 2, along with the results of the present experiments. In view of the sensitivity of the annealing response to experimental variables, (see p. 4 ) the agreement between these different investigations is satisfactory. Stage II accounts for a somewhat larger fraction of the total recovery in the present experiments than has been observed by Manintveld[46] or Jongenburger;[47] in addition, Stage V occurs at lower temperatures. These differences are consistent with the higher purity level of the silver used in this investigation. No indication of a distinct annealing stage in the temperature range corresponding to Stage III can be seen in the annealing spectrum (Fig. 7). Instead, the annealing which occurs between Stage II and Stage V appears to be continuous and cannot be characterized by a unique activation energy. This so-called "garbage annealing" which occurs over the temperature range from about 150° to 300°K, accounts for only about 15% of the total recovery. Stage IV was not detected here, probably because

Table 2. Recovery of the Electrical Resistivity of Cold-worked Silver

| Investigator | Purity | Deformation Conditions | | Annealing Response | | | |
|---|---|---|---|---|---|---|---|
| | | Type & amount | Temp. °K | Stages obs. | Temp. range, °K | % recovery | $E_{act.}$, eV |
| Ramsteiner, Schülle & Seeger[52] | 99.999% | Rolling, 50-85% | below * 230° | III | 230°- 260° | + | 0.60±0.05 |
| | | | | IV | 325°- 400° | | 0.88±0.05 |
| | | | | V | > 350° | | 1.0 - 1.4 |
| Jongenburger[47] | 99.998% | Tensile, 13-27% | 14° | II | 14°<—>180°x | 30 | not reported |
| | | | | III | 180°<—>300°x | 20 | |
| | | | | IV | 350° - 400° | 10 | |
| | | | | V | ~ 420° | 40 | |
| Manintveld[46] | ? | Tensile ? | 78° | II | 80°- 160° | 20 | 0.18 |
| | | | | III | 200°- 260° | 15 | 0.65 |
| Present work | 99.9999% | Tensile, 20% | 78° | II | 90°- 130° | 40 | 0.16±0.03 |
| | | | | V | 300°- 360° | 45 | —— |

* Rolled after cooling to 90°K; rolling temperature deduced from presence of frozen alcohol on specimen surface.

\+ Cannot be evaluated on an equivalent basis due to absence of Stage II.

x Specimens annealed only at 14°, 180°, and 300°K.

it was obscured by the onset of recrystallization (i.e., by Stage V). It should be noted that, using stored energy measurements, van den Beukel[48] has recently observed two major stages in the recovery of silver deformed at 78°K. These stages occurred in the same temperature ranges as those reported by Manintveld,[46] and the activation energies were in agreement with those derived from resistivity data.

The fact that Stage II in the recovery of the electrical resistivity is not accompanied by any observable recovery of the flow stress (see Fig. 10) is taken as evidence that this stage involves the annihilation of point defects, as was first emphasized by Molenaar and Aarts.[49] A recovery stage with an estimated activation energy of 0.2±0.05 eV has also been observed in this same temperature range (80-170°K) after irradiation.[50,51] According to Ramsteiner et al.[52], Stage II in irradiated silver is due to the recombination of relatively widely spaced interstitial-vacancy pairs, as distinguished from Stage I which is believed to be associated with the recombination of neighboring Frankel pairs. However, various other interpretations have been offered[6,7] and it is by no means established that Stage II after deformation occurs by exactly the same processes as those in irradiated materials, since the initial concentrations as well as the spatial distribution of vacancies and interstitials may be quite different in these two cases.

A summary of the annealing characteristics of pure silver, the Ag-0.1 at. % Mg alloy, and the oxidized alloys is presented in Table 3. The major effect of magnesium in solid solution is to shift Stage V toward higher temperatures by about 100°K, i.e., to delay the onset of recrystallization. This may be attributed to the retarding influence which impurities exert on the migration of high-angle boundaries.[53] There is a mild indication of an annealing stage between about 260° and 320°K which could possibly correspond

Table 3. Summary of the Annealing Characteristics

| Material | Stage | Temp. Range, °K | % Recovery | | Activation energy, eV |
|---|---|---|---|---|---|
| | | | Elect. Resistivity | Flow Stress | |
| 99.9999% Ag | II | 90°- 130° | 40 | 0 | 0.16±0.03 |
| | contin. annealing | 130°- 300° | 15 | 5 | ——— |
| | V | 300°- 360° | 45 | 85 | ——— |
| Ag 0.1 at.% Mg | II | 90°- 130° | 30 | 0 | 0.16±0.03 |
| | contin. annealing | 130°- 340° | 20 | 5 | ——— |
| | plateau* | 340°- 400° | (0) | 10 | ——— |
| | V | 400°- 470° | 45 | 80 | ——— |
| Ag 0.1 at.% Mg[1] | II | 200°- 260° | 15 | 0 | 0.16±0.03 |
| | plateau* | 260°- 360° | (0) | 5 | ——— |
| | contin. annealing | 360°- 550° | 20 | 15 | ——— |
| Ag 0.1 at.% Mg[2] | contin. annealing | 78°-550° | 25 | 15 | ——— |

(1) Oxidized as Recrystallized
(2) Oxidized as Cold Drawn
* See Figure 7

to Stage IV; however the annealing in this range could not be characterized by a unique activation energy. Stage II in the solid solution alloy accounts for a smaller fraction of the total recovery than in pure silver, which may be understood in terms of the interactions between solute atoms and point defects. Thus, magnesium atoms would be expected to trap point defects in their vicinity and prevent them from contributing to the recovery process.

The annealing response of the cold-worked oxidized alloys differs significantly from that of pure silver. Not only is recrystallization drastically inhibited but point defect annealing processes are also strongly retarded. Consider first the alloy oxidized in the recrystallized condition. A stage in the recovery of the electrical resistivity is observed in this material (from 200° to 260°K) which is not accompanied by any change in the flow stress. This stage may therefore be assigned to point defect annealing. The apparent activation energy for this stage is the same, within experimental limits, as that for Stage II in pure silver or the unoxidized alloy, indicating that the point defect annealing processes involved are similar in all three materials. However, this stage in the oxidized alloy accounts for only about 15% of the total recovery, as compared to 40% in pure silver, and is displaced toward higher temperatures.

It is suggested that this behavior is due to the trapping of point defects in the strain fields surrounding the Mg-O clusters. Trapping of this type would certainly be expected since it would lead to a reduction in the average strain energy. The binding energy between the clusters and point defects may, in fact, be quite appreciable. Point defects which are trapped in this manner might also be expected to retain their identity and thus contribute to the resistivity, rather than being completely annihilated. The idea that point defects produced by deformation may effectively retain their

identity even when trapped at dislocations has recently been introduced by Birnbaum[54] in order to explain the strain aging effects observed in copper at low temperatures. Since Stage II is much more pronounced in pure silver than in the oxidized alloy, it is concluded that the strain fields surrounding the Mg-O clusters provide far better trapping centers for point defects than do dislocations.

The parallel recovery of the resistivity and flow stress which occurs at temperatures above about 400°K in the oxidized alloys is indicative of dislocation annealing (compare Fig. 7 and 10). It is clear, however, that the rearrangement or annihilation of dislocations is greatly retarded by the strong interactions between dislocations and the dispersed Mg-O clusters. The detailed nature of these interactions cannot be specified since independent structural studies have not been carried out. It is possible, however, that the gradual annealing observed in the range above 400°K may correspond to small amounts of local recrystallization. Brimhall[55] has recently observed local recrystallization in internally oxidized Ag-Mg alloys by transmission electron microscopy, and evidence for this effect had previously been obtained by Klein[5] and Gorsuch.[33] The localized nature of the recrystallization process is readily accounted for in terms of the restraint which the oxide clusters offer to grain boundary migration.[4]

The alloy oxidized as cold drawn does not exhibit a well defined point defect annealing stage, as may be seen from Fig. 7. Only about 5% of the initial resistivity increment anneals out before any recovery of the flow stress is discernible. There are at least two possible ways of accounting for this behavior:

(1) Point defect trapping of the kind previously discussed is more effective in this material than in the alloy oxidized in the recrystallized condition; this could presumably be due to the higher average dislocation

density or to a real difference in the characteristics of the dispersed phase.

(2) As shown previously, the anomalous dependence of the resistivity increment on strain indicates that relatively fewer point defects are produced in this material during deformation; this may manifest itself more clearly on annealing.

It is not possible to distinguish between these two possibilities on the basis of present information. The situation may be clarified somewhat, however, by carrying out quenching experiments on these materials. If the rates with which quenched-in defects anneal out are substantially different in the oxidized alloys, as compared to pure silver, these differences might be ascribed fairly unambiguously to the trapping of vacancies by the Mg-O clusters. On the other hand, the interpretation of the quenching experiments would not be as straightforward as it might appear. For example, internal stresses would be generated by differential contraction during quenching, and these might be sufficient to nucleate dislocations around the clusters. Consequently, the contributions which the clusters (and their associated strain fields) make to the resistivity might be difficult to separate from the resistivity increment due to quenched-in vacancies.

## 5. SUMMARY AND CONCLUSIONS

The presence of a dispersed phase produced by internal oxidation of a dilute silver-magnesium alloy has been observed to inhibit recovery and recrystallization on annealing after low temperature deformation. The effect apparently arises both from the influence of the dispersed phase on the structure of the cold worked state and its influence on the subsequent annealing behavior of the defects generated by deformation. Although it was not possible to separate these effects with certainty on the basis of the present experiments, some conclusions may be drawn, namely:

(1) The presence of the dispersed phase results in an increased rate of defect production during deformation.

(2) The relative concentrations of dislocations and point defects generated by deformation appear to be controlled by the initial dislocation structure of the material and the detailed characteristics of the dispersed Mg-O clusters or zones, i.e., their size, spatial distribution, degree of coherency, etc.

(3) Point defect annealing is apparently inhibited by the trapping of vacancies and/or interstitials in the elastic strain fields surrounding the Mg-O clusters. The trapped defects appear to retain their identity and thus continue to contribute to the resistivity. It is suggested that the interactions between point defects, in particular vacancies, and Mg-O clusters might be studied in more detail by carrying out quenching experiments, from which an estimate of the binding energy between vacancies and clusters might be obtained.

(4) The dispersed phase provides obstacles to the climb and cross-slip of dislocations thus retarding dislocation rearrangement and

annihilation on annealing; the clusters also act to restrain the migration of grain boundaries and thereby inhibit recrystallization.

(5) Internal oxidation leads to a significant increase in the electrical resistivity, the yield stress and the work hardening rate of the silver magnesium alloy. These effects suggest that coherent Mg-O clusters or zones of very small dimensions (less than 30 Å diameter) are formed during oxidation. The resulting elastic strain in the silver matrix is believed to account for the magnitude of the observed resistivity increment, while the strengthening effects are ascribed to elastic interactions between glide dislocations and the strain fields surrounding the clusters.

## ACKNOWLEDGMENTS

The author wishes to acknowledge the advice and encouragement of Dr. Lawrence Himmel.

This work was done under the auspices of the U. S. Atomic Energy Commission through the Inorganic Materials Research Division of the Lawrence Radiation Laboratory.

BIBLIOGRAPHY


1. R. F. Bunshah and C. G. Goetzel, "A Survey of Dispersion Strengthening of Metals and Alloys," WADC Tech. Rept. 59-414 (1959).
2. J. L. Meijering and M. F. Druyvestyn, Philips Res. Rep. 2, 81, 200 (1947).
3. N. J. Grant and O. Preston, Trans. AIME, 209, 349 (1957).
4. A. Gatti and R. L. Fullman, Trans. AIME, 215, 762 (1959).
5. M. J. Klein, Ph.D. Thesis, Stanford University (1961).
6. H. G. van Bueren, Imperfections in Crystals, North-Holland, Amsterdam (1960).
7. R. W. Baluffi, J. S. Koehler and R. O. Simmons, in Recovery and Recrystallization of Metals, Interscience, New York-London (in press).
8. W. M. Lomer, Progr. Metal Phys., 8, 255 (1959).
9. P. R. Swann, "Dislocation Arrangements in Face-Centered Cubic Metals and Alloys," in Electron Microscopy and Strength of Crystals, Interscience, New York-London, p. 131 (1963).
10. M. F. Ashby and G. C. Smith, Phil. Mag. 5, 298 (1960); also M. F. Ashby, Ph.D., thesis, University of Cambridge (1961). (To be published).
11. R. W. K. Honeycombe, Progr. Matl. Sci., 9, 92 (1961).
12. A. Kelly, "Theories of Precipitation and Dispersion Hardening," in Electron Microscopy and Strength of Crystals, Interscience, New York-London, p. 947 (1963).
13. D. McLean, Mechanical Properties of Metals, J. Wiley and Sons, New York-London, p. 181 (1962).
14. G. Greetham, Ph.D., thesis, University of Sheffield (1959).
15. R. W. Guard, in Strengthening Mechanisms in Solids, ASM, Metals Park, Ohio, p. 253 (1962).

16. J. S. Lally, (to be published); quoted by P. B. Price, "Direct Observations of Glide, Climb and Twinning in Hexagonal Metal Crystals", in Electron Microscopy and Strength of Crystals, Interscience, New York-London, p. 80 (1963).

17. J. M. Arrowsmith, Ph.D. Thesis, University of Cambridge (1960).

18. E. Hornbogen, (unpublished); quoted by L. S. Darken, Trans. Quarterly 54, 599 (1961).

19. R. L. Fleischer, "Theory of Hardening by Thin Zones", in Electron Microscopy and Strength of Crystals, Interscience, New York-London, p. 973 (1963).

20. K. A. Jackson, Phil. Mag. 7, 1615 (1962).

21. E. Orowan, Symposium of Internal Stresses in Metals and Alloys, Inst. of Metals, London, p. 451 (1948).

22. J. C. Fisher, E. W. Hart, and R. H. Pry, Acta Met. 1, 336 (1953).

23. R. B. Nicholson, G. Thomas, and J. Nutting, J. Inst. Metals, 87, 429 (1959).

24. J. Weertman, J. Appl. Phys. 26, 1213 (1955); also U. S. Naval Research Lab Report #5123 (April 1958).

25. P. B. Hirsch, Phil. Mag. 7, 67 (1962).

26. J. Nutting, in Strengthening Mechanisms in Solids, ASM, Metals Park, Ohio, p. 78 (1962).

27. H. R. Peiffer, Trans. AIME, 221, 60 (1961).

28. H. G. van Bueren, Philips Res. Rep. 12, 190 (1957).

29. T. Federighi and G. Thomas, Phil. Mag. 7, 127 (1962).

30. M. B. Kasen and D. H. Polonis, Acta Met. 10, 821 (1962).

31. R. Resnick and L. Siegle, Trans AIME, 209, 87 (1957).

32. L. A. Girafalco and B. E. P. Beestom, Acta Met. 11, 161 (1963).

33. P. D. Gorsuch, Ph.D. Thesis, Rensselaer Polytechnic Institute (1956),

34. P. Fetta, unpublished research.

35. D. K. C. MacDonald, Handbuch der Physik, Springer-Verlag, Berlin Vol. 14, p. 137 (1956).

36. C. J. Meecham and J. A. Brinkman, Phys. Rev. 103, 1193 (1956).

37. L. S. Darken, Trans. Quarterly, 54, 599 (1961).

38. S. Weissman and D. F. Wreidt, unpublished; quoted by Darken, ref. 37.

39. D. Maher, unpublished research.

40. D. W. Pashley, Phil. Mag. 4, 316 (1959); also D. W. Pashley and A. E. B. Presland, in Structures and Properties of Thin Films, J. Wiley and Sons, New York, p. 199 (1959).

41. P. R. Swann and D. F. Wreidt, to be published; quoted by Darken, ref. 37.

42. W. Eichenauer and G. Müller, Z. Metallk. 53, 321 (1962).

43. D. Lazarus, Sol. State Phys. 10, 71 (1960).

44. L. M. Clarebrough, M. E. Hargreaves, and M. H. Loretto, in Recovery and Recrystallization of Metals, Interscience, New York-London (in press).

45. J. E. Bailey and P. B. Hirsch, Phil. Mag. 5, 485 (1961).

46. J. A. Manintveld, Nature, 169, 623 (1952).

47. P. Jongenburger, Acta Met. 9, 985 (1961).

48. A. van den Buekel, Physica, 27, 603 (1961).

49. J. Molenaar and W. H. Aarts, Nature, 166, 690 (1950).

50. J. W. Marx, H. G. Cooper, and J. W. Henderson, Phys. Rev. 88, 106 (1952).

51. R. M. Walker, Rendicotti della Scuola Internazionale de Fisica 'Enrico Fermi' (1960).

52. F. Ramsteiner, W. Schüle, and A. Seeger, Phys. Stat. Sol. 2, 1005 (1962); see also A. Seeger, in Radiation Damage in Solids, Vol. 1, International Atomic Energy Agency, Vienna, p. 101 (1962).

53. K. T. Aust and J. W. Rutter, Trans. AIME 215, 119 (1959); ibid 218, 50 (1960).

54. H. W. Birnbaum, J. Appl. Phys. (in press); ibid 32, 1403 (1961); 33, 750 (1962).

55. J. L. Brimhall, unpublished research.

This report was prepared as an account of Government sponsored work. Neither the United States, nor the Commission, nor any person acting on behalf of the Commission:

A. Makes any warranty or representation, expressed or implied, with respect to the accuracy, completeness, or usefulness of the information contained in this report, or that the use of any information, apparatus, method, or process disclosed in this report may not infringe privately owned rights; or

B. Assumes any liabilities with respect to the use of, or for damages resulting from the use of any information, apparatus, method, or process disclosed in this report.
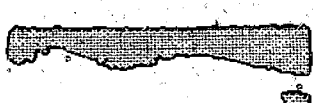
As used in the above, "person acting on behalf of the Commission" includes any employee or contractor of the Commission, or employee of such contractor, to the extent that such employee or contractor of the Commission, or employee of such contractor prepares, disseminates, or provides access to, any information pursuant to his employment or contract with the Commission, or his employment with such contractor.